



5th International Conference on Advances in Energy Research, ICAER 2015, 15-17 December 2015, Mumbai, India

Design, Simulation and Implementation of Current Fed Isolated Full Bridge DC-DC with Voltage Multiplier for Fuel Cell Grid Applications

Dr.D.Elangovan^{a,*}, M. Sai Krishna Reddy^a, Tania. H.M^a, Dr.R. Saravana Kumar^a

^a*School of Electrical Engineering, VIT University, Vellore-632014, India*

Abstract

This paper proposes novel current fed converter full bridge isolated DC-DC converter with voltage multiplier and active clamp circuit for fuel cell grid connected applications. The proposed converter is best suited for fuel cells and their interfacing to utility three phase grid. Active clamp concept introduced on the primary side of isolation transformer to reduce the turn-off voltage spikes of full bridge active devices. Innate soft-switching with elongated range can be achieved in the recommended converter by using the parasitic capacitance of MOSFET switches and leakage inductance of the high frequency transformer. Zero Voltage Switching(ZVS) is achieved for all the primary devices which allow greater switching frequency operation and improvement in over-all efficiency of the converter for utility interface. Cost, size and weight of the converter minimizes for the higher switching operation of the converter. Half-wave Cockcroft-Walton Voltage Multiplier (H-W C-W VM) having minimum number of multiplying stages is used on the secondary side of the designed converter in order to get the required DC-link voltage for three phase utility grid connection. The converter's switching frequency is maintained at 100 KHz. This paper is organized as introduction, steady state operation, simulation results with two different cases i.e. full load and half load conditions and finally, test result validation of a 250 Watt experimental setup with the proposed converter.

© 2016 The Authors. Published by Elsevier Ltd. This is an open access article under the CC BY-NC-ND license (<http://creativecommons.org/licenses/by-nc-nd/4.0/>).

Peer-review under responsibility of the organizing committee of ICAER 2015

Keywords: Active clamp;current-fed;Voltage multiplier;ZCS;Fuel cell

* Corresponding author. Tel.: 91-9894207260;
E-mail address: elangovan.devaraj@vit.ac.in

1. Introduction

Today’s technology is mainly looking at sustainable energy. Though we have several renewable technologies available for different power applications, some constraints on existing topologies are not able to give promising solutions. Out of all the available renewable sources, fuel Cells are considered to be more capable and standard power generating units as fuel cells supply power as long as fuel supply is there. Lesser voltage at the output of stack, dull response to load variations, presence of ripple current which slashes down the efficiency and permitting reverse current flow are the disadvantages associated with fuel cell, inspire of it being a promising power solution. To overcome the above technical challenges very strong power conditioning unit should be present. To connect fuel cell with utility grid we need to develop a power converter with high voltage gain.

More-over fuel cell characteristics differ from other renewable sources characteristics. This characteristic has three regions of operation as shown in Fig.1. These regions are very important in deciding converter operating set point for maximum power extraction from the fuel cell[1].

Current fed converters are best suitable for fuel cells. Current fed topologies either full bridge or half bridge isolated DC-DC converters have given appropriate solutions for most of the technical challenges faced by fuel cells [2]. Full bridge current fed isolated DC-DC converters were analyzed in [3, 4]. These converters and their complete analysis were given in [5, 6]. Active clamp concept was introduced in current fed converter topologies to reduce the turn-off spikes of active switches to greater extent in [7, 8].

A current fed converter with active clamp ZVS and having a rectifier on the secondary side is analyzed completely in [9].This converter’s gain depends on the turn’s Ratio of the transformer which in turn causes increase in the magnetic size thereby reducing its power density.The proposed converter is shown in fig.2.The paper is organized as detailed analysis of steady state operation in 2nd section and simulation and experimental results proposed in 3rd section. Finally, conclusion and references are included.

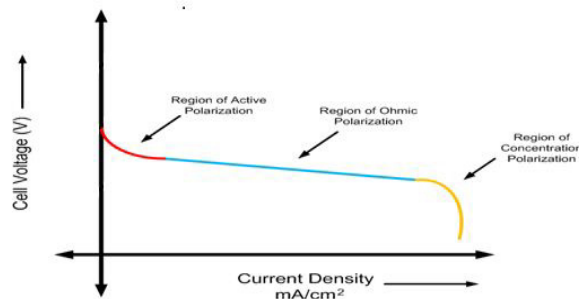


Fig.1 Characteristics of Fuel Cell at low temperatures.

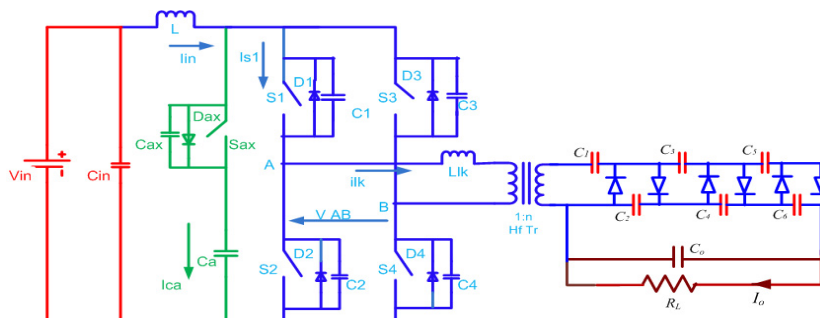


Fig.2 The proposed Current Fed converter with three stage multiplier

2. Steady State operation and analysis

In this section, complete analysis and steady state operation of the converter with design equations is presented. Main focus is given to the proposed converter with active clamp circuit and voltage multiplier. Mode by mode analysis with Active-Clamped ZVS operation was explained for one complete half cycle. Analysis is done on the primary side alone, due to the presence of voltage multiplier on the secondary of the high frequency transformer which just behaves as a multiplying stage. Fig.3 shows the Theoretical steady state operating waveforms of the proposed converter.

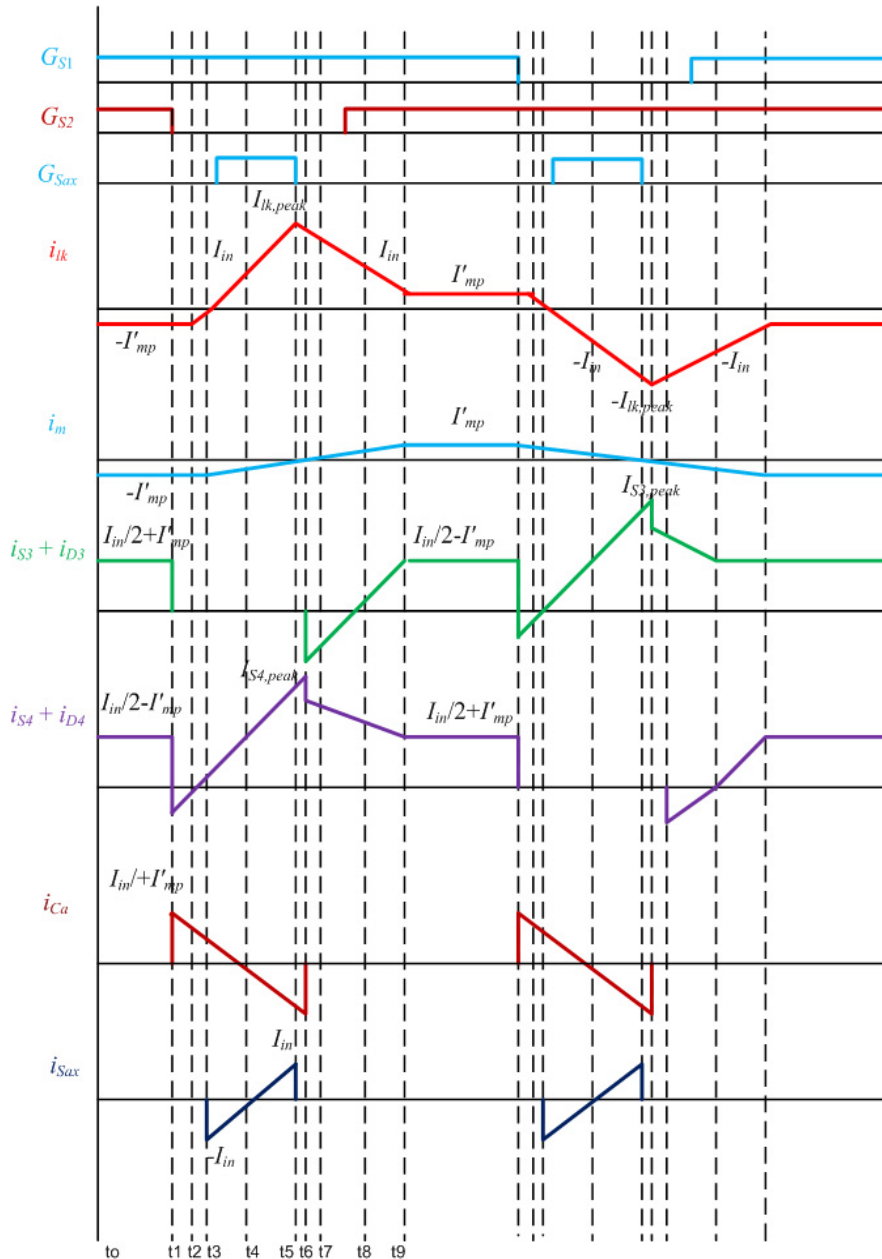


Fig.3. Theoretical Steady State operating Waveforms of the proposed converter

2.1.Interval 1($t_0 < t < t_1$)

In this interval, all the four switches on primary side S1 to S4 are turned ON and the Clamping Switch S_{ax} is turned OFF. Boost inductor starts storing energy. The transformer leakage inductance current flows through all the switches so that increment in currents of switches S1 and S4 occurs. Other two switch currents through S2 and S3 decreases. Fig.4(a) shows circuit equivalent of this interval.

$$i_{lk} = i_m = -i'_{mp} \tag{1}$$

$$i'_{mp} = \frac{V_{in}}{2 * f * (L_{lk} + L_m)} \tag{2}$$

$$V_{sax} = \frac{V_{in}}{2 * (1 - D)} \tag{3}$$

$$V_{cau} = \frac{V_{in}}{2 * (1 - D)} \tag{4}$$

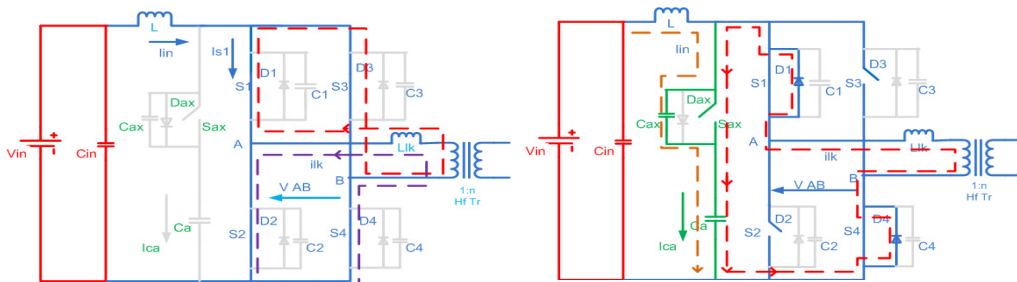


Fig. 4(a) Interval 1; (b) Interval 2

2.2.Interval 2($t_1 < t < t_2$)

In this interval at $t=t_1$ primary switches S2 and S3 are made to turn OFF by removing the pulse. Boost inductor current changes the path through the clamping switch which causes zero current through all the switches. Leakage current flows through the body diodes of D1 and D4 of primary MOSFET devices S1 and S4 respectively. Hence the current through switches S1 and S4 immediately dips to negative value. Parasitic capacitance of device C2 and C3 of primary MOSFET devices S2 and S3 gets charged and clamping switch capacitor C_{ax} gets discharged. Fig.4(b) shows the circuit equivalent of this interval.

$$V_{s2}(t_2) = V_{s3}(t_2) = \frac{V_0}{n * 2 * n_s} \tag{5}$$

$$V_{Sax} = V_{Ca} - \frac{V_0}{n * 2 * n_s} \tag{6}$$

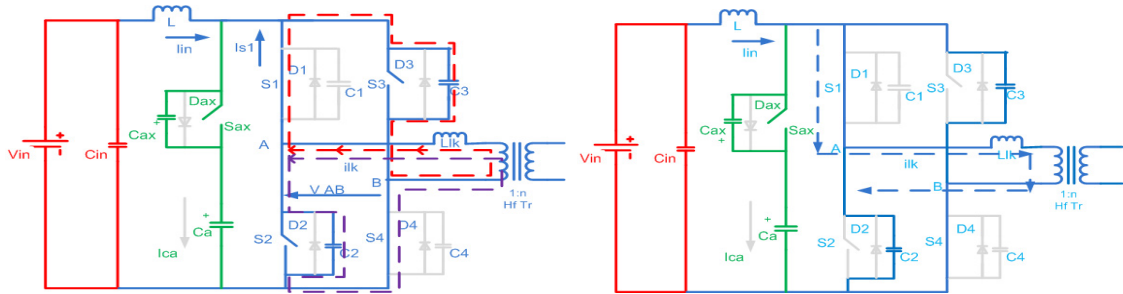


Fig.5 (a) Interval 3; (b) Interval 4

2.3. Interval 3 ($t_2 < t < t_3$)

At the end of this interval parasitic capacitances of C2 and C3 charges up-to V_{ca} and C_{ax} discharges to zero. The primary side switches voltages V_{s2} and V_{s3} have increased from V_0/n to V_{ca} . A positive voltage equal to $(V_{ca}-V_0/n)$ appears across the transformer leakage inductance and current through it, i_{lk} rises linearly. Leakage Current i_{lk} changes to positive which results in conduction of rectifying diodes D_{R1} and D_{R4} . This interval is very short and Fig.5(a) shows the equivalent circuit diagram of this mode.

$$i_{lk} = -I'_{mp} + \left(V_{s2} - \frac{V_0}{n * 2 * n_s} \right) / L_{lk} * (t - t_2) \tag{7}$$

$$i_m = -I_{mp} + \frac{V_0}{L_m} * (t - t_2) \tag{8}$$

$$i_{s1} = \frac{I_{in}}{2} - I'_{mp} + \frac{V_{s2} - \frac{V_0}{n * 2 * n_s}}{L_{lk}} * (t - t_2) \tag{9}$$

$$V_{s2}(t_3) = V_{c2}(t_3) = V_{ca}(t_3) = \frac{V_{in}}{2(1-D)} \tag{10}$$

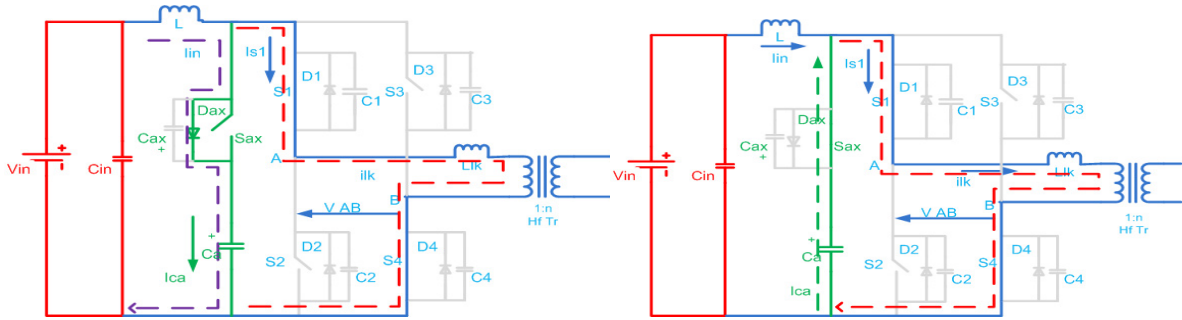


Fig.6 (a).Interval 5; (b) Interval 6

2.4. Interval 4 ($t_3 < t < t_4$)

In this interval body diode of clamping switch is made to conduct to ensure that voltage across the switch is zero for ZVS of clamping switch. Clamping capacitor C_a gets charged and the supply current flows through S1&S4. Fig.5(b) shows the circuit equivalent of this interval.

$$i_{lk} = i_{lk}(t_3) + \left(V_{ca} - \frac{V_0}{n * 2 * n_s} \right) / L_{lk} * (t - t_3) \tag{11}$$

$$i_{s1} = i_{s1}(t_3) + \frac{V_{ca} - \frac{V_0}{n * 2 * n_s}}{L_{lk}} * (t - t_3) \tag{12}$$

$$i_m = i_m(t_3) + \frac{V_0}{L_m} * (t - t_3) \tag{13}$$

$$i_{ca} = I_{ca,peak} - \frac{V_0}{L_{lk}} * (t - t_3) \tag{14}$$

2.5. Interval 5 ($t_4 < t < t_5$)

In this interval S_{ax} is gated for turning ON with ZVS and C_a discharges through clamping switch. Magnetizing current i_m increases with the same slope. Fig.6 (a) shows the circuit equivalent of this interval.

$$i_{lk} = I_{in} + \left(V_{ca} - \frac{V_0}{n * 2 * n_s} \right) / L_{lk} * (t - t_4) \tag{15}$$

$$i_{ca} = I_{in} - i_{lk} = -\frac{V_{ca} - \frac{V_0}{n * 2 * n_s}}{L_{lk}} * (t - t_4) \quad (16)$$

$$I_{s1,peak} = I_{in} - I_{mp} + \frac{V_0}{L_m * f_s} * (1 - D) \quad (17)$$

2.6. Interval 6 ($t_5 < t < t_6$)

The clamp switch S_{ax} is turned off at $t=t_5$. Current i_{lk} charges C_{ax} and discharges C_2 and C_3 . The leakage inductance L_{lk} resonates with snubber capacitors C_{ax} and $C_2 + C_3$. This interval is very short and Fig.6(b) shows the circuit equivalent diagram of this interval. $V_{sax}(t_6) = (V_{ca} - V_0/n)$, $V_{s2}(t_6) = V_0/n$.

2.7. Interval 7 ($t_6 < t < t_7$)

In this interval i_{lk} still discharges C_2 and C_3 charge C_{ax} in resonant fashion. By the end of this mode C_2 and C_3 completely discharges to zero and C_{ax} charges to initial value and Fig.7(a) shows the circuit equivalent of this interval.

2.8. Interval 8 ($t_7 < t < t_8$)

If i_{lk} still present even after completely C_2 and C_3 discharged it flows through the path of body diodes of S_2 and S_3 which results in ZVS turn on of the switches S_2 and S_3 and Fig.7(b) shows the circuit equivalent of this interval.

$$i_{lk} = I_{lk}(t_7) - \left(\frac{V_0}{n * 2 * n_s} \right) / L_{lk} * (t - t_7) \quad (18)$$

$$i_{D2} = i_{lk} - I_{in} \quad (19)$$

2.9. Interval 9 ($t_8 < t < t_9$)

In this interval S_2 and S_3 are turned ON with ZVS. In this interval, switches S_2 and S_3 are turned on with ZVS. Current i_{lk} is transferred to the switches S_2 and S_3 . The interval ends when current i_{lk} equals to the current i_m . Fig.8 shows the circuit equivalent of this interval.

$$i_{s2} = \frac{V_0}{n * 2 * n_s} * (t - t_8) \quad (20)$$

$$i_{s1} = I_{in} - \frac{V_0}{n * 2 * n_s} * (t - t_8) \quad (21)$$

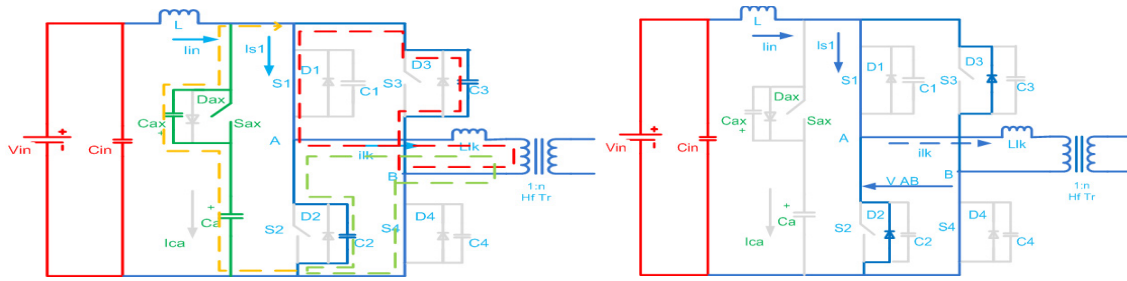


Fig. 7(a) Interval 7; (b) Interval 8

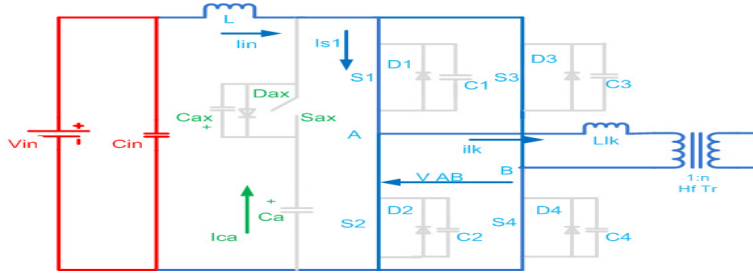


Fig.8. Interval 9

3. Design , Simulation and Experimental Results

The converter was designed by using the following design equations.

$$\text{Switch stress, } V_{sw} = \frac{V_0}{2 * n * n_s} = 40V \tag{22}$$

$$\text{Overlap Duty, } D_c = 2D - 1 = 0.44 \tag{23}$$

$$\text{Output voltage, } V_0 = \frac{V_{in} * n * n_s}{(1 - D)} \tag{24}$$

$$\text{Boost Inductor, } L = \frac{V_{in} * D_c}{\Delta i * 2 * f_s} = 0.45 \mu H \tag{25}$$

Multiplier Design

$$\text{Gain } X = \frac{V_0}{E_{pk}} \tag{26}$$

Where, V_0 = Output voltage

E_{pk} = Transformer secondary peak voltage.

Optimum number of stages is given by,

$$a_4n^4 + a_3n^3 + a_2n^2 + a_1n + a_0 = 0 \quad (27)$$

Where,

$$a_4 = 0 \quad (28)$$

$$a_3 = 1 \quad (29)$$

$$a_2 = -\frac{2.X - 3}{3} \quad (30)$$

$$a_1 = -\frac{9.X - 2}{12} \quad (31)$$

Using the above equations, optimum number of stages was calculated to be 3 (n=3).

Stage capacitances are calculated as follows , (n=3)

$$C_{2i} = C_{2i-1} = (n+1-i)C \quad (32)$$

$$C_{tot,min} = \frac{g}{f} \cdot \frac{n^2 \cdot (n+1) \cdot (2n+1)}{2 \cdot (2n-X)} \quad (33)$$

$$n(n+1)C = C_{tot,min} \quad (34)$$

C1 and C2 values are equal to 2.2 μ F ,C3 and C4 values are equal to 1 μ F and C5 and C6 values were calculated to be 0.47 μ F.[10]

Simulation results were considered for two cases for wide load variation. Results presented for full load and half load conditions with the following specifications of Table.1 which best suited for fuel cell interface with 3 phase grid connected applications.

Hardware implementation done with 250 watts and the results are shown from Fig.18 to 20. Fig.18 shows prototype, Fig.19 shows input voltage and current and Fig.20 shows the soft switching results. Experimental efficiency of 93.4 % achieved for the converter for different load conditions.

Table 1.Common simulation parameters for different cases.

Simulation Parameters	Values Full load	Values Half load
Input Voltage	22V	28V
Output Voltage	720 V	720V
Power Output	1000W	500W
Load Resistance	520 ohms	1037 ohms
Transformer turns ratio	1:3	1:3
Operating frequency	100 kHz	100 kHz

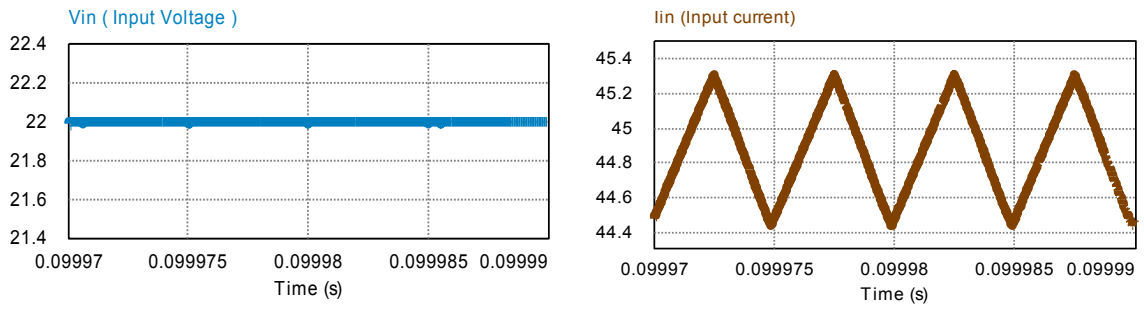


Fig. 9(a) Input voltage in full load ; (b) Input current in full load

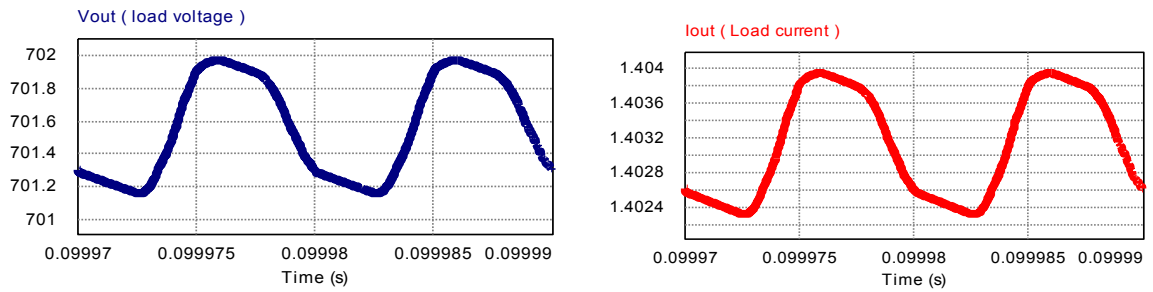


Fig. 10 (a) output voltage in full load ; (b) Output current in full load

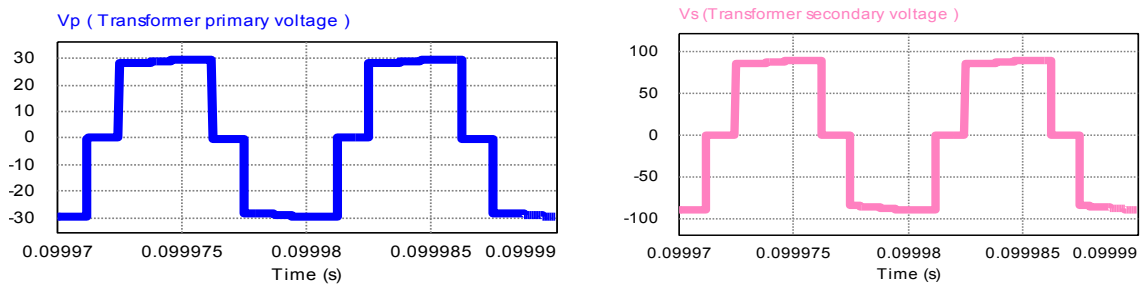


Fig. 11 (a) Transformer primary voltage in full load; (b) Transformer secondary voltage in full load

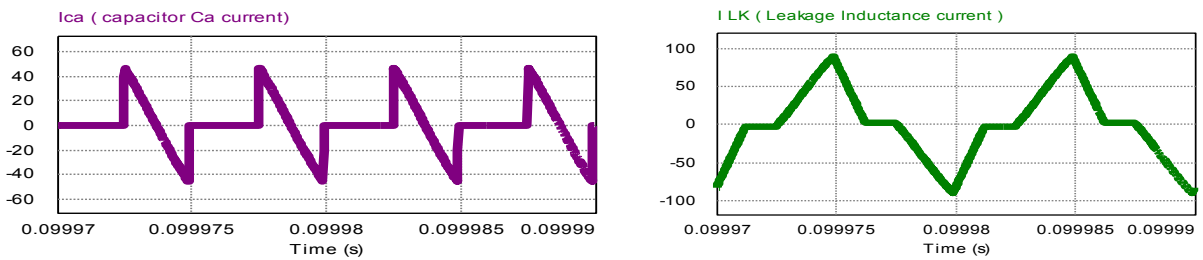


Fig. 12 (a) Capacitor C_a current in full load ; (b) Leakage Inductance current in full load

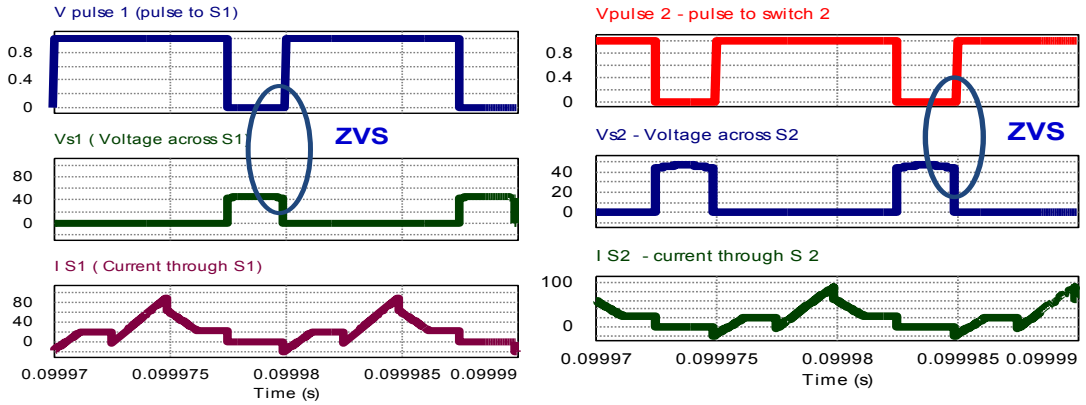


Fig.13 (a) Soft switching in switch 1 in full load ; (b) Soft switching in switch 2 in full load

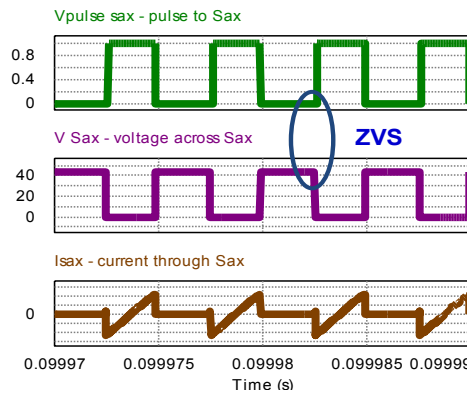


Fig. 14 Soft switching in switch Sax (auxiliary switch) in full load

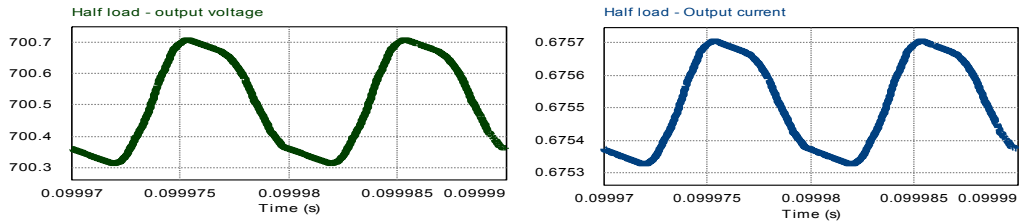


Fig. 15 (a) output voltage in half load; (b) Output current in half load

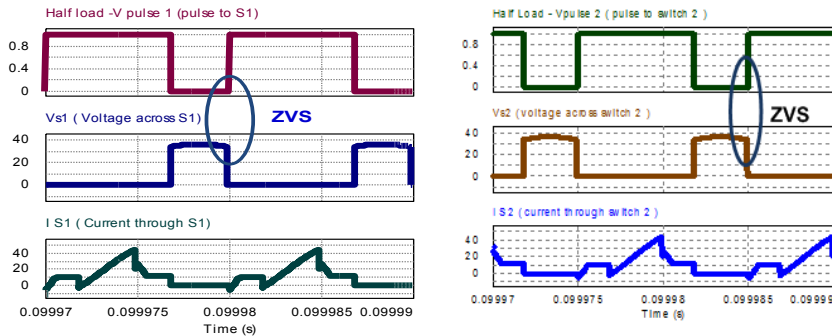


Fig.16(a) Soft switching in switch 1 in half load; (b) Soft switching in switch 2 in Half load

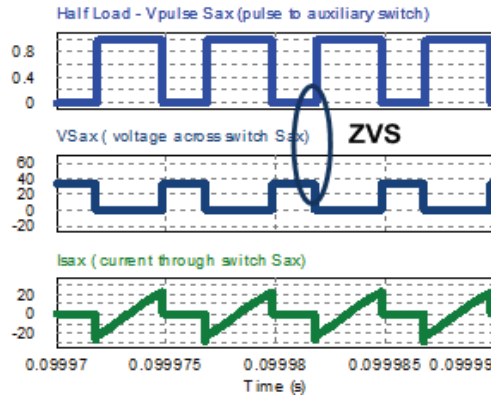


Fig. 17 Soft switching in switch Sax (auxiliary switch) in half load

From the soft switching waveforms, we can observe that soft switching is obtained for all the switches during half load as well as full load conditions. The switch pulse is turned on only when the voltage across the switch is zero (ZVS). When the body diode starts conducting, the switch pulse is given which can be observed from the current waveform which becomes negative as shown in Fig.13 to Fig .17.This ZVS turn on reduces the losses thereby improving the efficiency.

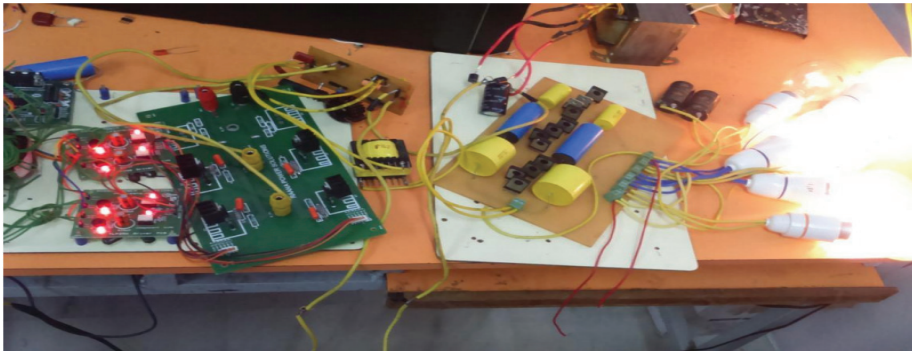


Fig.18. Hardware prototype model

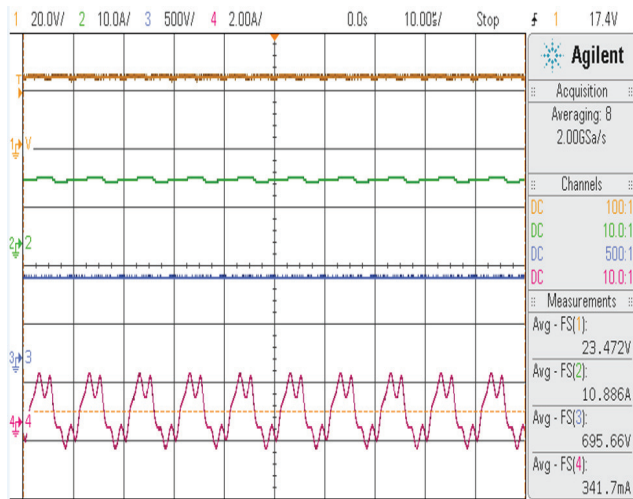


Fig.19. Input voltage, Input current, Output voltage and Output current

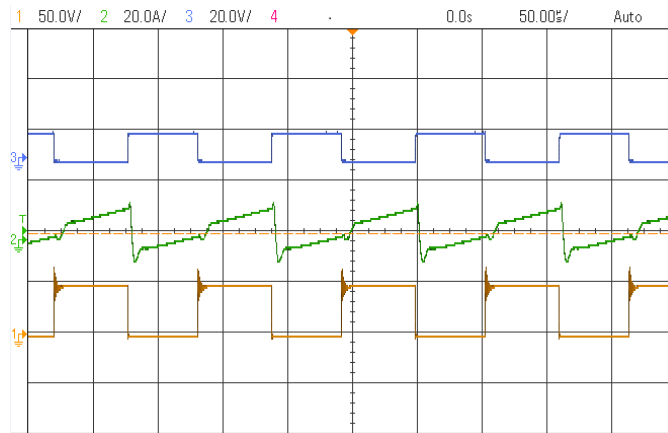


Fig20. Soft switching (ZVS) waveforms

4. Conclusion

Novel current fed full bridge dc-dc converter topology with voltage multiplier on the secondary side for the fuel cell interface with three phase utility grid was proposed. Design, simulation results and experimental results for the proposed converter are presented in different section. DC link voltage (700V) for three phase utility grid was generated using proposed converter with 250watt prototype model. Experimental efficiency of 93.4% was achieved and the proposed converter is best suitable for fuel cell as the ripple in input current is very low from the hardware results. Moreover the proposed converter was simulated and tested for different load conditions to validate the wide range operation of the converter for different fuel cell stack voltages as shown in figure-1 in introduction.

References

- [1] Akshay K Rathore. Interleaved Soft Switched active clamped L-L type current fed half bridge DC-DC converter for fuel cell applications. *International Journal of Hydrogen energy*, vol 34, 2009, pp 9802-9815.
- [2] D. Elangovan, R. Saravanakumar, Siddhartha Nigam. Design and Implementation of soft switched high gain Current Fed full bridge DC-DC converter for fuel cell applications. *Energy procedia-54*, 2014, pp 246-259.
- [3] X. Kong, L.T. Choi, AM. Khambadkone. Analysis and control of isolated current-fed full bridge converter in fuel cell system. In: Annual Conference of the IEEE Industrial Electronics Society (IECON'06); Nov 2006. p. 2825–30.
- [4] X. Kong, AM. Khambadkone. Analysis and implementation of a high efficiency interleaved current-fed full bridge converter for fuel cell system. *IEEE Transactions on Power Electronics* March 2007;22(2):543–50.
- [5] V. Yakushev, V. Meleshin, S. Fraidlin. Fullbridge isolated current-fed converter with active clamp. In: *IEEE APEC99*; March 1999. vol. 1. p. 560–66.
- [6] M. Mohr, FW Fuchs. Current-fed full bridge converters for fuel cell systems connected to the three phase grid. In: Annual Conference of the IEEE Industrial Electronics Society (IECON'06); Nov. 2006. p. 4313–8.
- [7] Jin-Tae Kim, Byoung-Kuk Lee, Tae-Won Lee, Su-Jin Jang, Soo-Seok Kim, Chung-Yuen Won. An active clamping current-fed half-bridge converter for fuel-cell generation systems. In: *Proceedings of IEEE Power Electronics Specialists Conference (PESC'04)*; 2004. p. 4709–14.
- [8] S. Han, H. Yoon, G. Moon, M. Youn, Y. Kim, K. Lee. A new active clamping zero-voltage switching PWM current-fed half bridge converter. *IEEE Transactions on Power Electronics* 2006;20:1271–9.
- [9] Akshay K Rathore, U.R. Prasanna. Analysis and design of zero-voltage-switching current-fed isolated full-bridge Dc/Dc converter. *IEEE Ninth International Conference on Power Electronics and Drive Systems (PEDS)*, 2011. pp. 239 – 245.
- [10] Ioannis C. Kobougias and Emmanuel C. Tatakis (2010), Optimal Design of a Half-Wave Cockcroft-Walton Voltage Multiplier With Minimum Total Capacitance, *IEEE Transactions On Power Electronics*, Vol. 25, No. 9, pp.2460-2468.